# In-plane and out-of-plane anisotropic magnetoresistance in $Ni_{80}Fe_{20}$ thin films

Th. G. S. M. Rijks* and S. K. J. Lenczowski†
*Department of Physics, Eindhoven University of Technology, P.O. Box 513, 5600 MB Eindhoven, The Netherlands and Philips Research Laboratories, Prof. Holstlaan 4, 5656 AA Eindhoven, The Netherlands*

R. Coehoorn
*Philips Research Laboratories, Prof. Holstlaan 4, 5656 AA Eindhoven, The Netherlands*

W. J. M. de Jonge
*Department of Physics, Eindhoven University of Technology, P.O. Box 513, 5600 MB Eindhoven, The Netherlands*
(Received 6 March 1997)

The anisotropic magnetoresistance (AMR) has been measured for $Ni_{80}Fe_{20}$ thin films, with the magnetization vector rotating in the film plane as well as out of the film plane. The out-of-plane (OP) AMR is found to be considerably larger than the in-plane (IP) effect, and strongly dependent on the degree of texture. In untextured films, the difference between the IP- and the OP-AMR is explained in terms of a dimensionality effect, whereas in (111)-textured films an additional contribution to the OP-AMR is found.
[S0163-1829(97)01025-4]

## I. INTRODUCTION

Many ferromagnetic materials and alloys exhibit the so-called anisotropic magnetoresistance (AMR) effect, which is manifested in the dependence of the resistivity on the angle between the current and magnetization direction. This effect, discovered in 1857 by Thomson,[1] is of technical interest in the field of magnetic recording.[2,3] The size of the effect is expressed by the AMR ratio, defined as $\Delta\rho/\rho \equiv (\rho_{\parallel}-\rho_{\perp})/\rho_{\parallel}$, in which $\rho_{\parallel}$ and $\rho_{\perp}$ are the resistivities with the magnetization parallel and perpendicular to the current direction, respectively. Large AMR ratios are found in bulk crystals of transition-metal alloys, such as $Ni_{70}Co_{30}$, for which $\Delta\rho/\rho$ equals about 27% at 4.2 K and 6–7 % at room temperature.[4] In magnetic sensing devices based on the AMR effect often thin films with the approximate composition $Ni_{80}Fe_{20}$ are used. $Ni_{80}Fe_{20}$ (Permalloy) combines a very small cubic magnetocrystalline anisotropy with a very small magnetostriction constant. In addition, it is possible to induce a small in-plane uniaxial anisotropy in thin permalloy films by deposition in a magnetic field, leading to almost hysteresis-free hard-axis loops.[5] These properties, combined with a fair AMR ratio at room temperature, make Permalloy very suitable for sensor applications.

Usually the AMR effect is measured with the magnetization vector rotating in the film plane. We will call this the in-plane (IP) AMR effect. For a 30 nm thick $Ni_{80}Fe_{20}$ film an AMR ratio of typically 2% is measured at room temperature. Recently, semiclassical calculations of the resistivity and the AMR effect of thin films have been performed, for a rotation of the magnetization from the direction parallel to the current to the direction perpendicular to the current, in the film plane as well as perpendicular to the film plane. The latter effect will be called the out-of-plane (OP) AMR effect. From the calculations, the OP-AMR is expected to be considerably larger than the IP-AMR,[6] which is ascribed to a dimensionality effect. Marsocci[7] and Chen[8] have performed AMR measurements of Ni films with the magnetic field perpendicular to the current direction, varying the angle between the magnetic-field direction and the film plane from 0 to 90°. In polycrystalline Ni films with thicknesses of 47.8 and 107.5 nm, they found that the OP-AMR ratio is larger than the IP-AMR ratio. Although the authors recognized the presence of a dimensionality effect, the dependence of this effect on the angle between the magnetization vector and the film plane could not be explained by the theories of AMR, known at that time. In addition, measurements of (100)-oriented single-crystal films (with thicknesses of 68 and 107.5 nm), showed a marked dependence of the AMR ratio on the crystal axes along which the current and the magnetic field were aligned. This dependence has also been reported by several other authors,[9–12] for Ni and Ni-Fe single crystals. Viret *et al.*[13] have measured a 0.2 % lower OP resistance as compared to the IP resistance ($\mathbf{M}\perp\mathbf{I}$) in a 30 nm polycrystalline Co film. They explained this effect by assuming that upon the application of a perpendicular magnetic field domain walls, which in the near-zero field state give rise to an additional contribution to the resistivity analogous to the giant magnetoresistance in magnetic multilayers, are eliminated.

In this paper we will present the results of both IP- and OP-AMR measurements on sputter-deposited Permalloy films, with thicknesses varying from 4.5 to 100 nm. We will show that the OP-AMR ratio is indeed considerably larger than the IP-AMR ratio. By studying the IP- and OP-AMR effects in untextured as well as textured films as a function of film thickness, combined with a careful analysis of the structural properties of these films, we have been able to clearly demonstrate the dimensionality effect. Using the description of the AMR effect, as proposed in Ref. 6, we are now able to explain the dimensionality effect, that was measured in 1964.[7,8] Unfortunately, the large OP-AMR effect in $Ni_{80}Fe_{20}$ films is unlikely to be applied in future magnetic field sensors because of the large field necessary to overcome demagnetization.

 © 1997 The American Physical Society

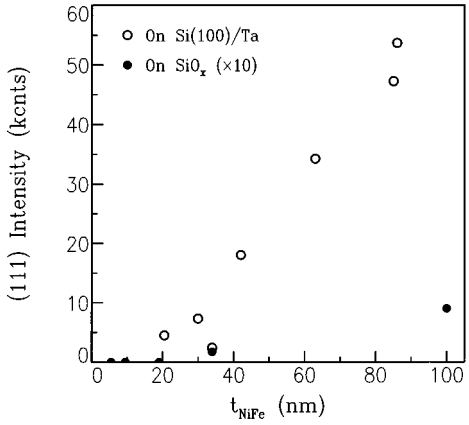


FIG. 1. (111)-peak intensity of the high-angle XRD spectra as a function of the $Ni_{80}Fe_{20}$ layer thickness. Note that the peak intensities of the layers grown on $SiO_x$ are multiplied by a factor of 10.

## II. EXPERIMENT

Samples were prepared by dc magnetron sputtering at a base pressure of $5\times10^{-9}$ Torr and an argon pressure of $5\times10^{-3}$ Torr (target-substrate distance is 110 mm). As substrates, $4\times12$ mm$^2$ Si(100) single crystals and also thermally oxidized Si were used. The single-crystal substrates were precleaned by an *ex situ* 2% HF dip to remove the oxide skin. $Ni_{80}Fe_{20}$ films, with thicknesses varying from 4.5 to 100 nm, were grown on Si(100) using a 3 nm Ta buffer layer as well as directly on the $SiO_x$ substrates (no buffer). Deposition rates were about 0.2 nm/s. Layer thicknesses were calibrated using low-angle x-ray diffraction (XRD). During deposition a magnetic field was applied along the long axis of the sample, which induces a small uniaxial anisotropy in $Ni_{80}Fe_{20}$.

High-angle XRD has revealed a strong (111) texture in the films sputtered on Si(100)/Ta, whereas the films sputtered on $SiO_x$ only show a very weak (111) texture for films thicker than about 35 nm and essentially no texture at all for thinner films. Figure 1 shows the XRD (111) peak intensity as a function of film thickness, for the films grown on Si(100)/Ta and on $SiO_x$. The full width at half maximum of the XRD rocking curves is typically 3-4° for the films grown on Si(100)/Ta and 20° for the films on $SiO_x$. A 3 nm Ta layer has been deposited on top of both types of samples, in order to prevent the $Ni_{80}Fe_{20}$ layer from oxidation. Cross-sectional transmission electron microscopy (TEM) has shown that the films are polycrystalline. The films grown on Si(100)/Ta show a columnar grain structure, whereas in the films grown on $SiO_x$, the grains do not exhibit this kind of columnar shape.[14] Plan-view TEM experiments have been performed on films, sputter-deposited on $Si_3N_4$ windows. In order to validate a comparison of the grain structure of Ta/$Ni_{80}Fe_{20}$/Ta films grown on both Si(100) and $Si_3N_4$, grazing-incidence XRD was used. With this technique the average lateral grain size can be estimated from the peak width using Scherrer's law.[15] The measurements did not show any significant difference between the films grown on Si(100) and $Si_3N_4$. The (111)-textured films exhibit a random in-plane crystallite orientation. A TEM study on the influence of a Ta buffer layer on the microstructure of a 30 nm $Ni_{80}Fe_{20}$ film has shown that application of a Ta buffer layer results in an increase of the grain size.[16] From a detailed analysis of plan-view TEM micrographs of $Ni_{80}Fe_{20}$ films, grown on a 3 nm Ta buffer layer, we derived an average lateral grain size of about 12 nm for a $Ni_{80}Fe_{20}$ thickness of 30 nm. For a film without a Ta buffer layer we estimate an average lateral grain size of about 8 nm.[16] This is in good agreement with Ref. 14.

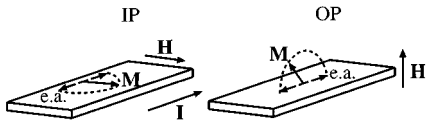


FIG. 2. Schematic view of the sample-field configurations. The easy axis (e.a.) of the induced anisotropy is directed along the long axis of the sample. The magnetic field is applied perpendicular to the easy axis, either in-plane (IP) or perpendicular to the film plane (OP).

Resistance measurements were performed at 5 K in a setup with four contacts in-line. The two different field configurations, are shown in Fig. 2: (i) the IP configuration, with the magnetic field in the film plane along the hard magnetization axis, i.e., perpendicular to the uniaxial anisotropy axis and (ii) the OP configuration, with the field perpendicular to the film plane. In both configurations, the magnetization is expected to rotate coherently. The sample is mounted on a goniometer in order to realize an accurate orientation with respect to the magnetic field. The current is directed in the film plane along the long (easy) axis of the sample. The resistance is measured in an ac mode with a frequency of 13 Hz. Therefore a possible misalignment of the voltage contacts does not result in the measurement of a Hall voltage in the OP configuration.

## III. RESULTS AND DISCUSSION

Figure 3 shows the results of two typical measurements of the sheet resistance $R_\square$ as a function of the magnetic field $H$, (a) in the IP and (b) in the OP configuration. In saturation, the magnetization is perpendicular to the current resulting in a low resistance. The in-plane saturation field is less than 1 kA/m, determined by the uniaxial anisotropy. The perpendicular saturation field is about 840 kA/m, determined by demagnetization. The zero-field state is a state of high resistance, as the magnetization is parallel or antiparallel to the current due to the uniaxial anisotropy. In both cases, the field dependence of the resistance shows, to a good approximation, a parabolic behavior as is expected for the AMR when the magnetization rotates coherently. In that case the resistance change is proportional to $[1-(H/H_A)^2]$, in which $H$ is the applied field and $H_A$ is the anisotropy field determined either by the induced anisotropy (a) or demagnetization (b). In order to observe this behavior it is necessary, especially in the OP configuration, to align the magnetic field very carefully with respect to the sample. As is illustrated in Fig. 4, a misalignment of the field of about 2° from the film normal provides an in-plane field component of $0.035\cdot H$ that induces an in-plane rotation of the magnetization (in the field

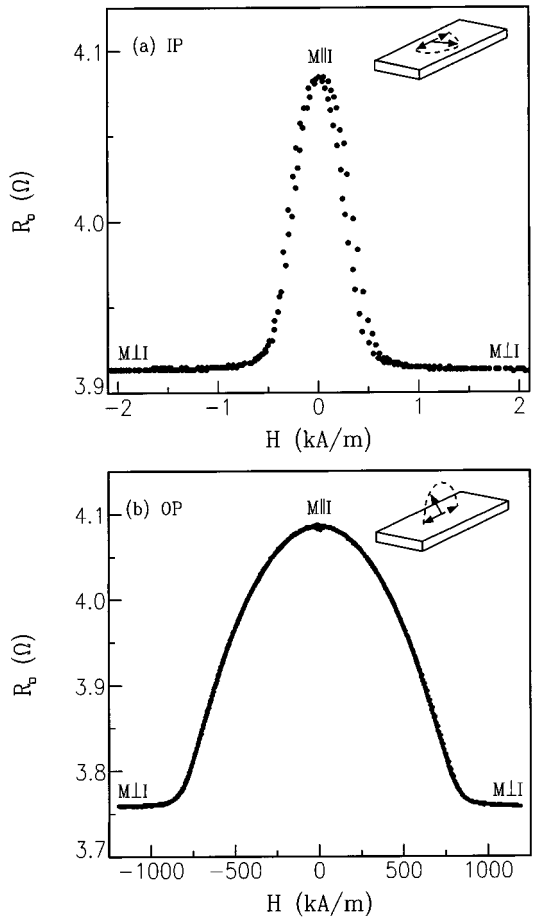


FIG. 3. Typical sheet resistance $R_\Box$ versus field $H$ curves of a 30 nm $Ni_{80}Fe_{20}$ layer, measured with the magnetic field (a) in the film plane (IP) and (b) perpendicular to the film plane (OP), at 5 K. At zero-field the magnetization is parallel or antiparallel to the current (**M**∥**I**), at large positive or negative fields the magnetization is perpendicular to the current (**M**⊥**I**).

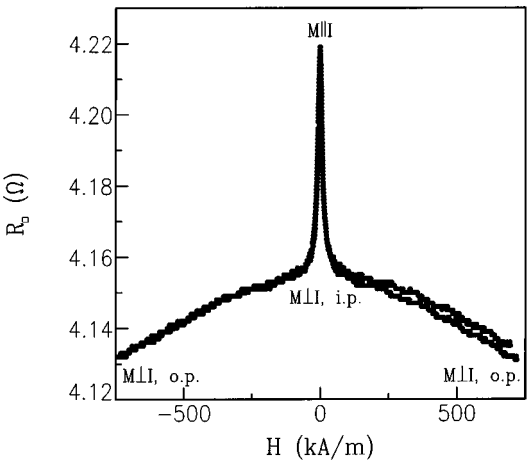


FIG. 4. Sheet resistance $R_\Box$ versus field $H$ curve, measured at 5 K in the out-of-plane (OP) configuration, with the field slightly misaligned (2° off normal). The small in-plane field component induces an in-plane (i.p.) rotation of the magnetization preceding the magnetization rotation out of the film plane (o.p.).

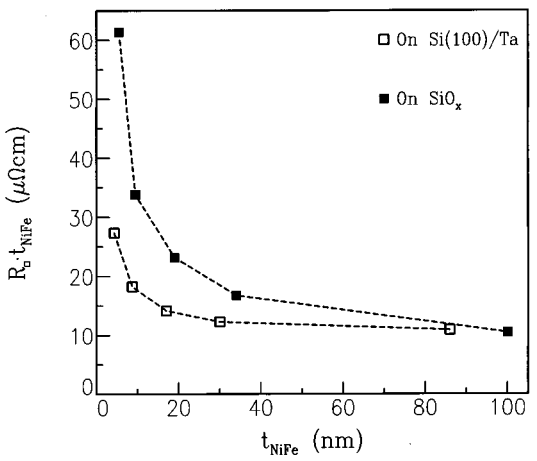


FIG. 5. The product of the sheet resistance and the $Ni_{80}Fe_{20}$ layer thickness $R_\Box \cdot t_{NiFe}$ as a function of $t_{NiFe}$, measured at 5 K for the textured (on Si(100)/Ta) and untextured (on $SiO_x$) films. The lines are guides to the eye.

range below 30 kA/m) preceding the magnetization rotation out of the film plane.

In Fig. 5 the product $R_\Box \cdot t_{NiFe}$, measured with the magnetization parallel to the current, is displayed as a function of the $Ni_{80}Fe_{20}$ layer thickness $t_{NiFe}$. The sheet resistance of the untextured films is, for small film thicknesses, considerably higher than that of the textured films but saturates to the same thick-film value of $10\mu\Omega$ cm. A systematic investigation of the relation between the degree of texture, expressed in the intensity of the XRD (111) peak reflection, and the resistivity showed a monotonic decrease of the resistivity with increasing (111) peak intensity.[17] This is ascribed to a decreasing influence of grain-boundary scattering with an increasing degree of texture. Because of the high resistivity of Ta ($\rho = 175\ \mu\Omega$ cm), the contribution of the Ta-buffer layer to the total film conductivity is less than 5%, so the effect of current shunting through the Ta-buffer layer is negligible. In Fig. 6(a) the AMR ratio $(\rho_\parallel - \rho_\perp)/\rho_\parallel$ in the IP configuration in the case of textured (open squares) and untextured films (filled squares) is shown as a function of $t_{NiFe}$. Fig. 6(b) shows the same in the OP configuration. A number of authors already demonstrated that the IP-AMR ratio depends on the film thickness (e.g., Refs. 4,18), which implies that a size effect in the *resistivity* depends on the orientation of the magnetization with respect to the current direction. Figure 6(a) shows that the IP-AMR ratio is only weakly dependent on the degree of (111) texture. In addition, the OP-AMR ratio is found to be always larger than the IP-AMR ratio and strongly dependent on the degree of (111) texture.

In an earlier paper[6] we have predicted a difference between the IP- and OP-AMR ratios due to a size effect, i.e., as a result of diffusive film boundary scattering. The AMR effect is calculated using the Boltzmann transport equation, assuming that the electron mean free path is spin dependent and anisotropic, i.e., depending on the angle between the electron velocity vector and the magnetization. For the specific example of dilute NiFe films (see Ref. 6 for the parameters used) the IP- and $\overline{\text{OP}}$-AMR ratios have been predicted to be different by 20–40 % for film thicknesses in the range of 1–10 nm. The difference disappears, of course, in the

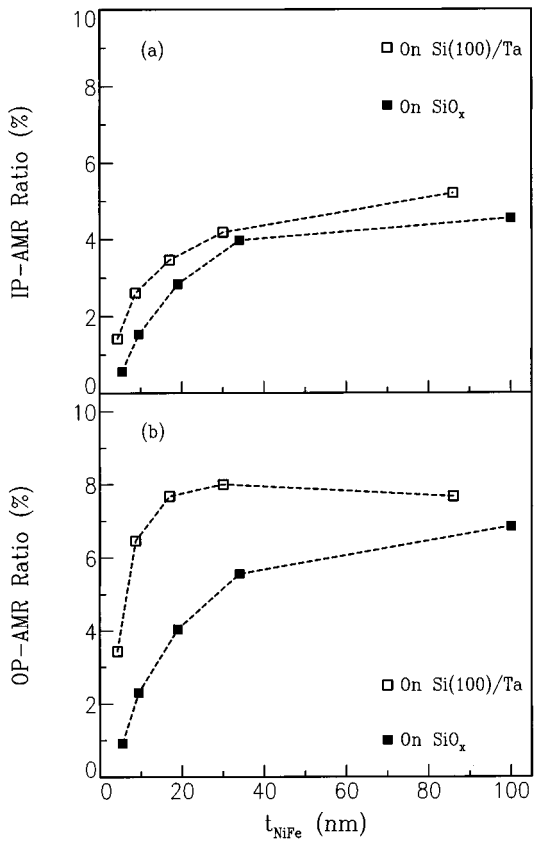


FIG. 6. AMR ratio as a function of the film thickness $t_{\mathrm{NiFe}}$, measured at 5 K for the textured (on Si(100)/Ta) and untextured (on $SiO_x$) films, in the (a) in-plane (IP) case and (b) out-of-plane (OP) case. The lines are guides to the eye.

limit of a thick film, when the film thickness becomes larger than the longest of the majority- or minority-spin mean free path, since then diffusive boundary scattering becomes negligible. This dimensionality effect may be understood as follows. Let us define a coordinate frame with the film normal in the $\hat{\mathbf{z}}$ direction, and the current in the $\hat{\mathbf{x}}$ direction. We will compare contributions to the conductance of electrons with two different velocity directions, within the $xy$ and $xz$ planes, respectively, but both with a given angle $\vartheta$ with respect to the $\hat{\mathbf{x}}$ direction. For the sake of clarity, this is illustrated in Fig. 7. In addition, we restrict ourselves to discussing the contribution of electrons of a single spin direction to the current, and assume that the scattering probability is largest for electron velocities parallel or antiparallel to the magnetization direction. This provides a good description for the case of NiFe (see Ref. 6, and references therein) and is also expected to be valid for Permalloy. In bulk crystals, neglecting a possible anisotropy in the transport properties related to the crystal symmetry, the contributions of the two velocity directions are equal if $\mathbf{M}\|\hat{\mathbf{x}}$ [Fig. 7(a)], and the *sum* of the two contributions is the same for $\mathbf{M}\|\hat{\mathbf{y}}$ and $\mathbf{M}\|\hat{\mathbf{z}}$ [Figs. 7(b) and 7(c)]: there is no difference in the IP- and OP-AMR ratio. However, in thin films the contribution to the conductance of electrons with a velocity vector in the $xz$ plane is decreased by the diffusive scattering at the film boundaries. This reduction is smaller when $\mathbf{M}\|\hat{\mathbf{z}}$, as compared to the situation with $\mathbf{M}\|\hat{\mathbf{y}}$. In the former case the mean free path of

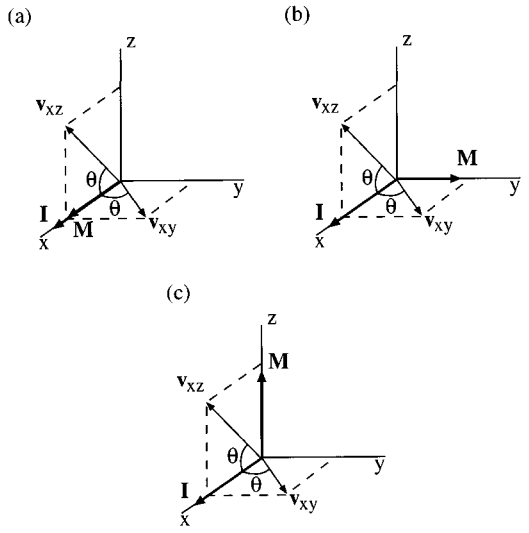


FIG. 7. Coordinate frames used to clarify the dimensionality effect. $\mathbf{v}_{xy}$ and $\mathbf{v}_{xz}$ are the velocity vectors within the $xy$ and $xz$ plane, respectively, both with an angle $\vartheta$ with respect to the $\hat{\mathbf{x}}$ direction.

electrons with a velocity vector in the $xz$ plane is smaller than in the latter case, due to the anisotropic scattering, which makes these electrons less sensitive to film boundary scattering. On the other hand, for electrons with velocities in the $xy$ plane there is no film thickness effect in their contribution to the conductance. As a result, the net effect is that the conductance for the situation $\mathbf{M}\|\hat{\mathbf{z}}$ is larger than in the case of $\mathbf{M}\|\hat{\mathbf{y}}$ (and both conductances are still larger than for $\mathbf{M}\|\hat{\mathbf{x}}$), and therefore the OP-AMR ratio is larger than the IP-AMR ratio.

The experimental results that we have presented clearly support the prediction that the OP-AMR ratio is larger than the IP-AMR ratio due to the dimensionality effect. However, it must be remarked that in realistic systems there are two complicating aspects, that affect the difference between the OP- and IP-AMR ratios. First, the resistance not only depends on the angle between the current and magnetization vectors, but also on the orientation of these vectors with respect to the crystal axes. This has been observed for Ni and Ni-Fe single crystals,[7–12] and both phenomenological and microscopic theories within which this effect may be described have been discussed in Refs. 9, 12, and 19. This effect may provide an alternative explanation for the difference between the OP- and IP-AMR ratio of the (111)-textured films grown on Si(100)/Ta, which is considerably larger than in the case of the untextured films grown on $SiO_x$. We expect, however, that the dimensionality effect discussed above is still responsible for part of the difference between the OP- and IP-AMR in the textured films. In the untextured films, grown on $SiO_x$, we attribute the difference between the OP- and IP-AMR ratios entirely to the dimensionality effect. We note that in the case of the untextured films, the IP- and OP-AMR ratios would be expected to be equal in the thick-film limit. Experimentally, however, a difference remains. This may be explained by the presence of a weak (111) texture in the thickest films on $SiO_x$, as was measured by XRD (Fig. 1). The second complicating effect

is grain-boundary scattering. It has been demonstrated in Ref. 20 that grain boundaries are an important source of electron scattering in sputter-deposited Permalloy films, similar to those investigated in the present study, even up to large film thicknesses. It leads to a thick-film value of the AMR ratio which is considerably smaller than the value of 16% (at 4.2 K), obtained for bulk systems.[4] The slightly lower IP-AMR ratio for the untextured films is attributed to a different grain structure as compared to the textured films,[14,16] resulting in a more pronounced grain-boundary scattering of the electrons. This can, however, not explain the large difference in OP-AMR ratios. A complicating aspect of grain-boundary scattering is that it depends on the film thickness, as grain diameters vary with the film thickness.[20,21] Although good progress has been made in Ref. 20 in relating grain-boundary scattering to the microstructure, we will, in view of the microstructural complications involved, not attempt in the present paper to quantitatively analyze the variations with film thickness of the difference between the OP- and IP-AMR ratios.

## IV. CONCLUSIONS

We have carried out a systematic study of the anisotropic magnetoresistance in both strongly (111)-textured and untextured polycrystalline $Ni_{80}Fe_{20}$ thin films, with the magnetization vector rotating in the film plane as well as out of the film plane. Accurate orientation of the samples with respect to the field yields parabolic resistance versus field loops, indicating a coherent rotation of the magnetization. The OP-AMR ratio is found to be considerably larger than the IP ratio, and, in addition, strongly dependent on the degree of texture. In untextured films, the difference between the IP- and OP-AMR ratios is explained in terms of a dimensionality effect, whereas in textured films an additional contribution to the OP-AMR is found that is related to the orientation of the magnetization along a well defined crystal axis, i.e., the [111] axis perpendicular to the film plane.

## ACKNOWLEDGMENTS

The authors wish to thank A.E.M. De Veirman for the TEM analysis of our films. This research is part of the European Community ESPRIT3 Basic Research Project, Study of Magnetic Multilayers for Magneto-resistive Sensors (SmMmS) and was supported by the Technology Foundation (STW).

*Present and permanent address: Philips Research Laboratories, Prof. Holstlaan 4, 5656 AA Eindhoven, The Netherlands.

†Present and permanent address: Océ Nederland B.V., Department T-GR3, P.O. Box 101, 5900 MA Venlo, The Netherlands.

[1] W. Thomson, Proc. R. Soc. London **8**, 546 (1857).

[2] F. W. Gorter, J. A. L. Potgiesser, and D. L. A. Tjaden, IEEE Trans. Magn. **MAG-10**, 899 (1974).

[3] D. A. Thompson, L. T. Romankiw, and A. F. Mayadas, IEEE Trans. Magn. **MAG-11**, 1039 (1975).

[4] T. R. McGuire and R. I. Potter, IEEE Trans. Magn. **MAG-11**, 1018 (1975).

[5] M. S. Blois, Jr., J. Appl. Phys. **26**, 925 (1955).

[6] Th. G. S. M. Rijks, R. Coehoorn, M. J. M. de Jong, and W. J. M. de Jonge, Phys. Rev. B **51**, 283 (1995).

[7] V. A. Marsocci, J. Appl. Phys. **35**, 774 (1964).

[8] T. T. Chen and V. A. Marsocci, J. Appl. Phys. **43**, 1554 (1972).

[9] W. Döring, Ann. Phys. (Leipzig) **32**, 259 (1938).

[10] S. Marcus and D. N. Langenberg, J. Appl. Phys. **34**, 1367 (1963).

[11] W. A. Reed and E. Fawcett, J. Appl. Phys. **35**, 754 (1964).

[12] L. Berger and S. A. Friedberg, Phys. Rev. **165**, 670 (1968).

[13] M. Viret, I. Auneau, and J. M. D. Coey, J. Magn. Magn. Mater. **140-144**, 683 (1995).

[14] P. Galtier, R. Jerome, and T. Valet, in *Polycrystalline Thin Films, Structure, Texture, Properties, and Applications*, edited by K. Barmak, M. A. Parker, J. A. Floro, R. Sinclair, and D. A. Smith, MRS Symposia Proceedings No. 343 (Materials Research Society, Pittsburgh, Pennsylvania, 1994), p. 417.

[15] D. G. Neerinck, M. H. J. Slangen, A. E. M. De Veirman, Th. G. S. M. Rijks, and J. C. S. Kools, Thin Solid Films **280**, 136 (1996).

[16] A. E. M. De Veirman (unpublished).

[17] J. P. W. B. Duchateau (unpublished).

[18] E. N. Mitchell, H. B. Haukaas, H. D. Bale, and J. B. Streeper, J. Appl. Phys. **35**, 2604 (1964).

[19] V. A. Marsocci, Phys. Rev. **137**, A1842 (1965).

[20] Th. G. S. M. Rijks, R. L. H. Sour, D. G. Neerinck, A. E. M. De Veirman, R. Coehoorn, J. C. S. Kools, M. F. Gillies, and W. J. M. de Jonge, in Proceedings INTERMAG′95 [IEEE Trans. Magn. **31**, 3865 (1995)].

[21] A. F. Mayadas, J. F. Janak, and A. Gangulee, J. Appl. Phys. **45**, 2780 (1974).